

## Wet chemical surface functionalization of oxide-free silicon

Peter Thissen, Oliver Seitz and Yves J. Chabal\*

Department of Materials Science and Engineering, University of Texas at Dallas,  
800 West Campbell Road, Richardson, TX 75080, USA

\* corresponding author: [chabal@utdallas.edu](mailto:chabal@utdallas.edu)

### Abstract

Silicon is by far the most important semiconductor material in the microelectronic industry mostly due to the high quality of the Si/SiO<sub>2</sub> interface. Consequently, applications requiring chemical functionalization of Si substrates have focused on molecular grafting of SiO<sub>2</sub> surfaces. Unfortunately, there are practical problems affecting homogeneity and stability of many organic layers grafted on silicon oxide (SiO<sub>2</sub>), such as silanes and phosphonates, related to polymerization and hydrolysis of Si-O-Si and Si-O-P bonds. These issues have stimulated efforts in grafting functional molecules on oxide-free Si surfaces, mostly with wet chemical processes. This review focuses therefore directly on wet-chemical surface functionalization of oxide-free Si surfaces, starting from H-terminated Si surfaces. The main preparation methods of oxide-free H-terminated Si and their stability are first summarized. Functionalization is then classified into indirect substitution of H-termination by functional organic molecules, such as hydrosilylation, and direct substitution by other atoms (e.g. halogens) or small functional groups (e.g. OH, NH<sub>2</sub>) that can be used for further reaction. An emphasis is placed on a recently discovered method to produce a nanopattern of functional groups on otherwise oxide-free, H-terminated and atomically flat Si(111) surfaces. Such model surfaces are particularly interesting because they make it possible to derive fundamental knowledge of surface chemical reactions.

### Keywords

Silicon surfaces, hydrogen-termination, organic functionalization, self assembled monolayers, surface activation, nanopatterning

### Abbreviations

**Si**, silicon; **SiO<sub>2</sub>**, silicon oxide; **SAM**, self-assembled monolayer; **XPS**, X-ray photoelectron spectroscopy; **FT-IR**, Fourier transform infrared; **AFM**, atomic force microscopy; **NN**, nearest neighbor; **NNN**, next nearest neighbor; **RT**, room temperature; **TFT**, thin film transistor; **ALD**, atomic layer deposition; **MPA**, methylphosphonic acid; **ODPA**, octadecylphosphonic acid; **DFT**, density functional theory; **KMC**, kinetic Monte Carlo; **ML**, monolayer; **H**, hydrogen; **T-BAG**, tethering by aggregation and growth; **OH**, hydroxyl; **UHV**, ultra-high vacuum; **MOF**, Metal Organic Frameworks; **SURMOF**, surface Metal Organic Frameworks; **LBL**, layer-by-layer; **PL**, photoluminescence; **F**, fluorine;

## Content

1. Introduction
2. Oxide-free Si surfaces
  - 2.1. Formation of H-terminated Si surfaces
  - 2.2. Stability of H-terminated Si surfaces
3. Surface functionalization of oxide-free Si
  - 3.1. Indirect substitution
    - 3.1.1. Hydrosilylation
    - 3.1.2. Characterization of Si/SAM interfaces
  - 3.2. Direct substitution
    - 3.2.1. Halogen termination
    - 3.2.2. Amino termination
  - 3.3. Nanopatterning of Si(111) as a selective surface chemistry route
    - 3.3.1. Grafting 1/3 ML methoxy on H/Si
    - 3.3.1. Activating this nanopatterned, oxide-free Si surface
  - 3.4. Reactions on activated oxide-free Si(111) surfaces
    - 3.4.1. Phosphonation
    - 3.4.2. Metal-hydroxides
4. Concluding remarks and outlook
5. Acknowledgements
6. References

## 1. Introduction

Silicon has been dominating the microelectronic industry in part because it is plentiful and relatively cheap and can be produced with high purity, but mostly because of the chemical and electrical stability of the interface with its oxide.<sup>1,2</sup> In fact, the low concentration of electrical defect states at the Si/SiO<sub>2</sub> interface has been a strong driver to use Si for future devices such as electrical biosensors and photovoltaic components.<sup>1,2</sup>

Much work has therefore been devoted to modifying SiO<sub>2</sub> surfaces by grafting molecules via OH groups that typically terminate SiO<sub>2</sub> surfaces after wet chemical cleaning.<sup>3,4</sup> There are however two rather fundamental issues associated with modification of SiO<sub>2</sub> surfaces. The first is the very high activation energy for the reaction a number of species with surface OH groups, most notoriously for grafting phosphonic acid molecules.<sup>5</sup> The second is the poor chemical stability of the Si-O-Si bond at the interface between the organic layer and SiO<sub>2</sub>, due to facile hydrolysis under neutral or basic pH conditions.<sup>5</sup>

Two main methods have been used to functionalize SiO<sub>2</sub>. Silanization<sup>6,7</sup> has been the first method to graft organics to SiO<sub>2</sub>, but this method often suffers from the low surface OH group content of the Si surface oxide.<sup>3,4</sup> Indeed, comprehensive Si surface coverage by silanization derives from amorphous siloxane polymerization, and the degree of siloxane cross-condensation depends critically on the water content of the deposition solvent.<sup>7</sup> Attaining structural order in such films is also problematic.<sup>5</sup>

Alternatively, phosphonate molecules have been grafted on SiO<sub>2</sub> using a method called tethering by aggregation and growth or T-BAG.<sup>5</sup> During the T-BAG process, a phosphonic acid is initially weakly physisorbed from a solution onto the oxide substrate forming a reasonably well-ordered layer thanks to the interaction of the phosphonate headgroups of adjacent molecules, then chemically attached by a heating step, during which Si-O-P bonds are formed. The sample is then typically rinsed to remove any remaining physisorbed multilayers present on the surface on top of the chemisorbed SAM. T-BAG is a simple and reliable method to grow SAMs with phosphonate bonding on oxide surfaces. The physisorption step takes advantage of the organized arrangement of amphiphilic molecules at the liquid/gas interface, and is not restricted to specific environmental conditions like silanization reactions, which makes it potentially suitable for industrial applications. However, sample heating has been identified as a necessary condition of the T-BAG method to allow conversion of the physisorbed phosphonic acid to a chemisorbed phosphonate SAM, securing a monolayer to the surface prior to ultrasonic rinsing in water. This heating step and the prohibitively long time necessary to complete the chemical attachment (typically more than 48 h) are the two main disadvantages of this process.<sup>5,8</sup>

This process can be considerably shortened as recently shown by Vega et al.,<sup>8</sup> by controlling the humidity during the reaction time. While the T-BAG method leads to chemisorption, the quality of resulting films is not sufficient to derive a detailed bonding mechanism for phosphonates or to prevent subsequent degradation in aqueous solutions. Indeed, in contrast to the attachment of phosphonic acid to most of the metal oxides, the Si-O-P bond on SiO<sub>2</sub> is easily hydrolyzed, particularly in neutral or basic solutions typical in biological applications.

The issues outlined above for grafted silane or phosphonate molecules on SiO<sub>2</sub> have led to the modification of oxide-free Si surfaces by direct attachment of organic layers to Si. A driving force has been the relative ease in obtaining oxide-free surfaces by chemical removal of the

oxide in fluoride solutions (e.g. aqueous HF) leading to H-termination of the Si surface, as described in section 2.1.<sup>9</sup>

To better appreciate the issues associated with stabilizing Si surfaces with hydrogen for further chemical functionalization, it is useful to consider the formation process and the stability of H-terminated Si surfaces, as discussed in section 2.2.

The functionalization process consists therefore of transforming H-terminated Si surfaces into organically functionalized surfaces with formation of Si-X bonds at the interface. Prominent among these are metal complex catalyzed<sup>10</sup> or radical-induced hydrosilylation<sup>11-13</sup> of unsaturated organics (section 3.1). Electrochemical methods<sup>14,15</sup> or reactions with Grignard or lithium reagents are also effective for H-terminated Si<sup>16</sup>, although halogen-terminated Si surfaces can be used with organometallics<sup>17</sup> as well (section 3.2).

The recent finding that immersion of H-terminated Si(111) surfaces in neat anhydrous methanol at 65°C under controlled atmosphere leads to the slow formation of oxide-free methoxy-terminated surfaces<sup>18,19</sup> has stimulated much work because the methoxy groups (specifically 1/3 monolayer) are arranged in a well-defined pattern at the surface, with each methoxy center surrounded by six surface Si-H. The conditions required and the mechanism involved for achieving this nanopatterned surface are summarized in section 3.3.

The particular interest in this nanopattern is that the isolated methoxy centers can be activated by a series of simple steps to form Si-F, Si-OH or Si-(metal hydroxide) centers while remaining absolutely oxide-free (figure 1). The usefulness of such surfaces is illustrated in section 3.4 where further chemical functionalization with phosphonic acids and amino groups and details of metal hydroxide grafting are discussed.

Finally, this review highlights the importance of model surfaces, such as atomically flat yet chemically nanopatterned surfaces, for bringing a fundamental and microscopic understanding of surface chemistry by unraveling for instance the configurations of phosphonate bonding.

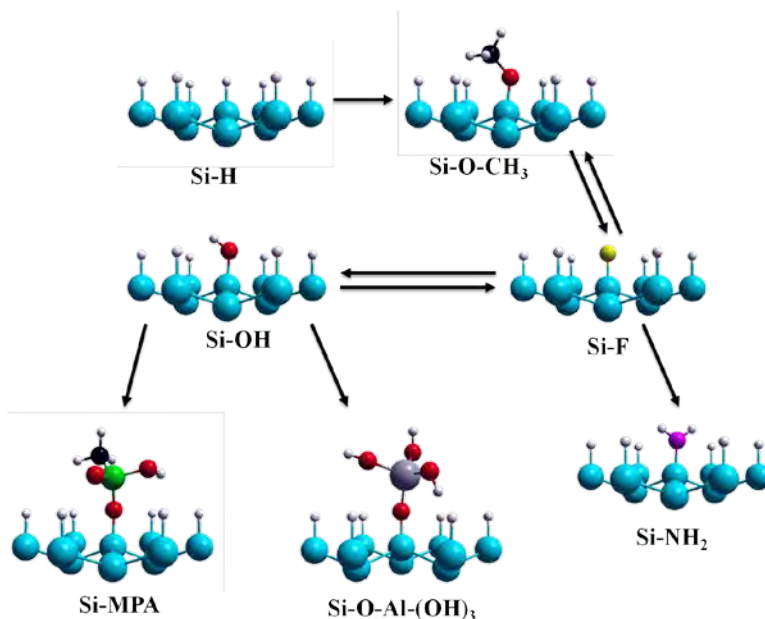


**Figure 1:** Overview of wet chemical reactions associated with nanopatterning: First,

partial reaction of a H-terminated Si(111) surface with methanol, then activation with HF to form Si-F, which can be transformed into OH by immersion in water or into NH<sub>2</sub> by immersion in NH<sub>3</sub>. The OH groups can be reacted with organic molecules or metal hydroxides. Si: blue, H: white, C: black, O: red, F: yellow, N: purple, Al: gray, P: green.

## 2. Oxide-free Si surfaces

### 2.1. Formation of H-terminated Si surfaces

It is now clear that HF-etched Si surfaces are H- and not F-terminated, as originally thought.<sup>20</sup> This conclusion is surprising because, as shown in the schematic figure 2, Si-F is formed as the last oxygen of the oxide is removed and the strength of the Si-F bond (~5.0 eV) is much higher than that of the Si-H bond (~3.5 eV).

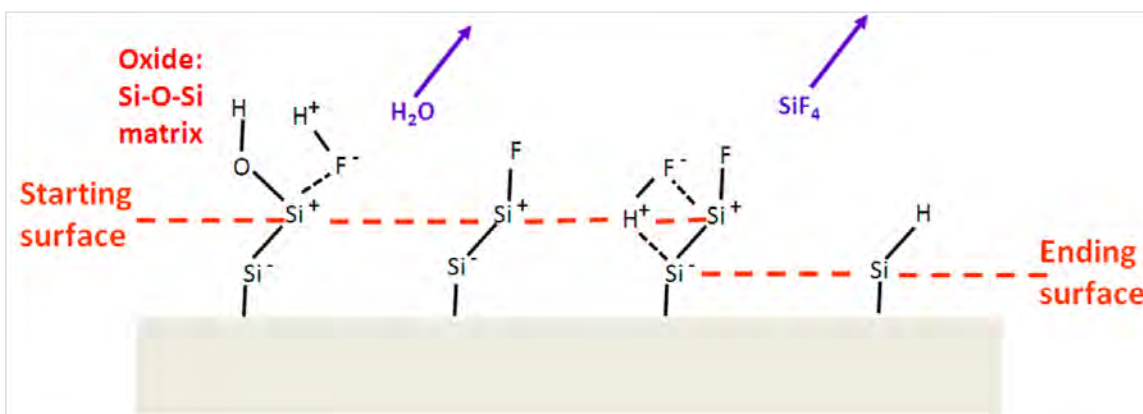


Figure 2: Mechanism leading to the formation of H-terminated Si surface by HF etching: The last step of oxygen removal from SiO<sub>2</sub> involves HF attack of the Si-O bond, with removal of OH as H<sub>2</sub>O and termination of the surface Si atom with fluorine. Further attack of the polarized Si<sup>δ-</sup>-Si<sup>δ+</sup> leads to H-termination.<sup>21</sup>

However, the strong polarization of the Si-Si back bond, due to the high electronegativity of fluorine, weakens this Si-Si bond and fosters the removal of the surface Si atom (onto which F is attached) in the form of SiF<sub>x</sub> molecules, leaving H-termination of the surface, as first proposed by Ubara *et al.*<sup>21</sup> on microcrystalline Si<sup>22</sup>, and later confirmed by experiments<sup>23</sup> and ab-initio calculations.<sup>24</sup> The resulting H-terminated surface is less polar and therefore quite resistant to further chemical attack by HF (i.e. there is no further etching in HF solution once the surface is H-terminated).

Recently, it was recognized that the above mechanism is dependent on the Si/SiO<sub>2</sub> interface structure. Indeed, the mechanism for HF etching described above is in fact only valid because the interface is rough, as schematically illustrated in figure 3.<sup>19</sup>

On an atomically rough surface (figure 3A), the F-terminated surface can be further attacked by HF to form a H-terminated surface because there is an atomic step, representing atomic roughness. On an atomically smooth surface (figure 3B), the intermediate Si-F species cannot be further chemically attacked because of steric hindrance and protection from the neighboring Si-H species, preventing access to the Si-Si backbonds.

While H-terminated surfaces are stable in HF (i.e. no further etching takes place), it is possible

by increasing the pH of the fluorinated solution (i.e. the OH<sup>-</sup> concentration through addition of basic buffers)<sup>9</sup> to selectively etch H-terminated surfaces, leading to very interesting structures: (i) atomically flat Si(111) surfaces (figure 4A),<sup>9</sup> and quasi-flat Si(100) surfaces (i.e. with well-defined bilayer structures), as illustrated in figure 4B and C.<sup>25</sup>

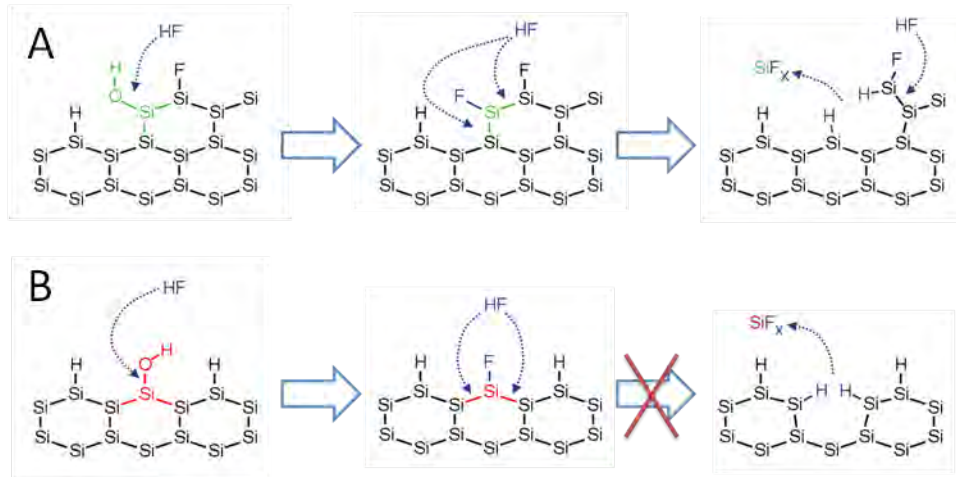


Figure 3: Mechanism of HF attack on (A) an atomically rough, partially F-terminated surface, and (B) an atomically flat, partially F-terminated surface.<sup>19</sup>

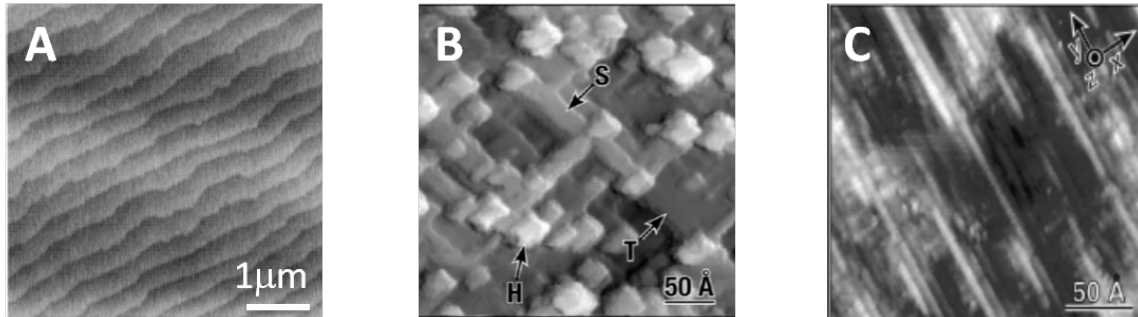


Figure 4: (A) Atomically flat H-terminated Si(111) surface, and (B and C) quasi-flat H-terminated Si(100) surfaces (i.e. with well-defined bilayer structures).<sup>26-28</sup>

Several studies<sup>26,29-32</sup> have suggested that the etching mechanism involves the OH<sup>-</sup> ions or related complexes with preferential removal of adstructures and attacks of steps, leading to highly structured surfaces such as atomically flat, monohydride-terminated Si(111) surfaces, or Si(111) surfaces with atomically straight steps.<sup>26,31</sup> Recent work performed on Si(100), however, has brought further insight into the mechanism, suggesting that the formation of silanone (Si=O) intermediate is a critical intermediate step in the etching process, leading to well-defined flat Si(100) surfaces (with double layer structures)<sup>33</sup> upon etching in NH<sub>4</sub>F. The overall mechanism proposed for the formation of atomically flat, monohydride-terminated surfaces is based on site-specific reactions,<sup>32</sup> leading to a step flow etching. The surface structure clearly plays a key role. The importance of surface structure has been emphasized here because it is central to surface

chemistry and therefore surface chemical functionalization, as will be illustrated in section 3.3. It is also important when considering the stability of H-terminated Si surfaces as summarized in the next section.

## 2.2. Stability of H-terminated Si surfaces

The relative stability and yet selective reactivity of H-terminated Si surfaces are essential components of the functionalization process, as summarized in this section. H-terminated Si surfaces undergo some degradation as soon as they become exposed to ambient air, only observable with charge recombination techniques. For instance, the surface recombination velocity increases by an order of magnitude when a Si sample is removed from an HF solution<sup>34</sup>, and some initial oxidation may be observed after several hours in some ambient atmospheres. Experiments performed in very well-controlled environments, however, have revealed that H-terminated Si surfaces are completely stable in pure gases (i.e. without radical contamination). Studies on flat and vicinal H-terminated Si(111) have shown for instance that reaction with O<sub>2</sub>, NH<sub>3</sub>, and H<sub>2</sub>O is initiated at steps, dependent on the step structure, and only takes place on flat terraces at temperatures above 300°C<sup>35</sup>. These findings indicate that, at RT (25°C), H-terminated Si surfaces are completely stable in clean gaseous environments even at atmospheric pressures. Degradation in air is therefore due to radicals, ozone or other reactive species that then leave the surface susceptible to oxidation.

Stability in solution is more complex because solvation effects can lower the reaction barriers since attempt frequencies are higher than those in vapor phase, and electrochemical effects can also enhance reactivity (hence the potential relevance of doping). For both gaseous and liquid environments, surface illumination can greatly modify the surface stability of H-terminated Si surfaces.<sup>11,36</sup>

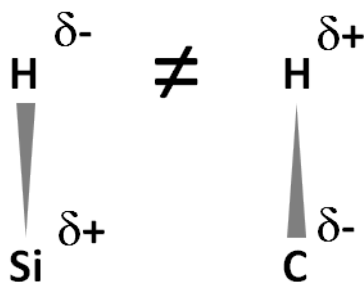


Figure 5: Dipole moment of Si-H vs. C-H bonding. Distribution of charge density is estimated on the base of electronegativity proposed by Pauling (H=2.20, C=2.55, Si=1.90).

Due to the low electronegativity of Si, the Si surface is partially oxidized by H-termination, leading to a small positive charge as shown in figure 5. Therefore, H-termination is similar to and can be discussed as hydrides (IUPAC: Silanes). Hydrogen has a relatively low electron affinity, and reacts exothermically with protons as powerful Lewis base (see figure 5 left). Himpsel *et al.* were the first to report in 1980 on geometry-dependent core-level shifts, in particular a positive shift of the first atomic layer in H-terminated Si(111)-(1x1) of 0.26 eV.<sup>37-39</sup>

### 3. Surface functionalization of oxide-free Si

#### 3.1. Indirect substitution

##### 3.1.1. Hydrosilylation

In 1993, Linford proposed a novel method for surface scientists that enabled the hydrosilylation of H-terminated Si whereby alkyl chains are covalently attached to Si(111) surfaces mainly by Si-C bonds.<sup>12,40</sup> This type of reaction has then been developed and reported in various reviews,<sup>41-44</sup> and more recently a large overview of the techniques for attachment and characterization of SAMs has been presented by Aureau et al.<sup>45</sup>

The essential element of hydrosilylation, summarized in equation (1), is the activation of the alkene, alkyne or other unsaturated carbon compounds to permit reaction with the Si-H surface.



For surfaces, the main advantage of the above reaction is the formation of thermodynamically and kinetically stable SAMs thanks to the strength and low polarity of the Si-C bond.

The three main forms of activation on surfaces include the use of catalysts or Lewis acids, intermediate halogenation of surfaces followed by Grignard chemistry, UV-light and temperature. The last two methods of activation are based on the use of a surface reaction and consequently are not derived from homogeneous hydrosilylation in solution that relies on a catalyst. Each approach has advantages and limitations, as briefly summarized below.

Catalysts and Lewis acid methods, originating from homogeneous liquid chemistry, have high yields but are prone to surface contamination by residual metallic catalysts or peroxide agents, often leading to Si surface oxidation.<sup>12,46-58</sup>

Replacement of hydrogen by halogens enables the attachment of short molecules, such as methyl groups that can be grafted as a full monolayer (100% coverage) on Si(111) surfaces.<sup>53,59</sup> However, the number of such graftable molecules is small and does not include molecules with another functional group, so the method is somewhat restrictive.

UV irradiation is powerful as it allows grafting of many types of molecules. The chemical reaction can proceed either through a radical-based mechanism or an exciton-based mechanism. Recently, work on diamond surfaces suggested that photoemission of electrons into the liquid could be responsible for producing radicals on acceptor molecules that could then catalyze the hydrosilylation of H-terminated carbon surfaces. The concept was subsequently carried over to Si substrates.<sup>60</sup> All the UV-induced processes are extremely sensitive to water contamination since water traces will easily react with the radicals formed on the surface to create SiO<sub>2</sub>. Consequently, they require the use of extremely anhydrous conditions and molecules, which is not easily available (particularly if a hydrophilic group is present on the molecules). On the other hand, photon-activated surface chemistry is ideally compatible with photolithographic processes, i.e. surface patterning.<sup>61-63</sup>

Thermal activation of hydrosilylation reactions is a straightforward alternative to chemical or photochemical activation. It is based on immersion of H-terminated Si surfaces in an anhydrous solution of appropriate alkenes at moderate temperatures (typically 150 to 200 °C). Although this thermal process is slow and therefore potentially sensitive to impurities, the solution temperature facilitates the removal of trace water, thus reducing the risk of surface oxidation. It also provides

thermal energy to suppress degradation on p-type Si<sup>64</sup> and promotes ordering of the layer. Therefore, simple methods and care in the execution of experiments make it possible to obtain surfaces with negligible interface oxide and high PL intensities (similar to H-terminated Si surfaces).<sup>65</sup> Such surfaces are significantly more stable than H-terminated surfaces once produced because of the protective SAM layer, even if the majority of the surface (e.g. 60-70%) is still H terminated. First performed in the 90's<sup>12,40</sup> and perfected for a number of unsaturated molecules,<sup>66,67</sup> thermal hydrosilylation was initially thought to involve surface radicals<sup>68,69</sup> or be due to trace impurities.<sup>69,70</sup> However, it is not clear how homolytic cleavage of a strong Si-H bond with bond energies on the order of 3.6 eV could occur at an appreciable rate at a temperature as low as 150°C. A more classical mechanism was therefore proposed<sup>71</sup> and calculated,<sup>72</sup> as illustrated in figure. 6.

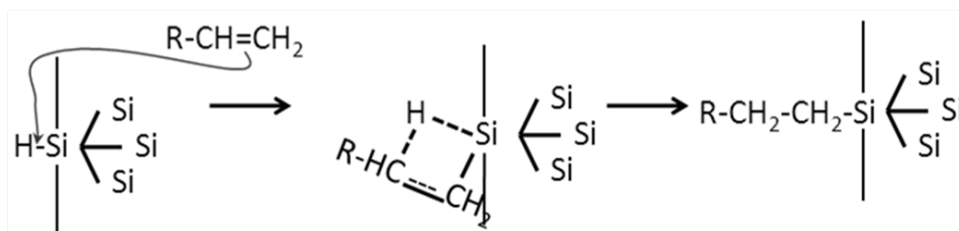


Figure 6: Possible reaction pathway for the concerted mechanism of the hydrosilylation.<sup>45</sup>

Both alkenes and alkynes have now been attached using thermal hydrosilylation, and quantitatively compared showing that triple bonds are preferentially attached over double bonds.<sup>73</sup> Furthermore, Scheres et al. have confirmed that an increased surface coverage is obtained with alkenyl chains on Si, compared to what can be achieved with alkyl chains.<sup>74</sup> Interestingly, in addition to the classical thermal method,<sup>69</sup> alkynes have also been grafted by very mild, RT methods in the dark,<sup>75</sup> producing better quality surfaces than alkenes.<sup>76</sup>

The thermal grafting methods were initially avoided partly for fear that thermal energy may activate the functional groups and induce them to react with Si-H instead of the unsaturated alkene terminus. Despite this potential problem, high-quality acid-terminated surfaces have been prepared by thermal grafting,<sup>77-79</sup> and used as anchor for metal-deposition,<sup>77</sup> biosensors<sup>79-82</sup> electrical contacts<sup>83,84</sup> or deposition of nanoparticles.<sup>78,85,86</sup>

### 3.1.2. Characterization of Si/SAM interfaces

To understand and control the indirect substitution reactions, a number of complementary characterization methods are important, such as contact angle measurements, spectroscopic ellipsometry, FT-IR, XPS and PL measurements. Electrical characterization and recombination time velocity measurements are the most sensitive methods to determine the density of electronic states at the Si/SAM interface. While the recombination time velocity has been measured for the simplest SAMs, such as methyl and ethyl layers, electrical measurements based on C-V and I-V measurements have been limited by the thickness of the SAM. To deal with this issue, an elegant approach has been developed by Peng et al.<sup>87</sup> using a high k dielectric (ALD deposited Al<sub>2</sub>O<sub>3</sub>) to increase the separation between the Si/SAM interface and the metallic top contact. Using this method, it was found that the density of states for the SAM-passivated Si(111) n-type surface after ALD treatment was in the order of  $2 \times 10^{11} \text{ cm}^{-2} \text{ eV}^{-1}$ , which is impressively low knowing

that for a thermally annealed equivalent Si/SiO<sub>2</sub> interface, the amount is  $1 \times 10^{11} \text{ cm}^{-2} \text{ eV}^{-1}$ .

### 3.2. Direct substitution

#### 3.2.1. Halogen termination

The main motivation for transforming H-terminated into halogen-terminated Si surfaces is a lower energy level of the transition states in consecutive reactions (lower reaction barriers). Hence, halogen termination (see figure 7) is used as starting point for a number of applications.

The chloro-terminated Si surfaces are prepared by treating the H-terminated Si (111) surfaces with PCl<sub>5</sub> at 80–100 °C using benzoyl peroxide as a radical initiator in chlorobenzene<sup>17,88</sup>. Other methods include (i) boiling Si wafer in chlorobenzene with PCl<sub>5</sub> and UV irradiation, and (ii) heating H-terminated Si at 80 °C in the presence of Cl<sub>2</sub><sup>89,90</sup>. Recently, high-quality halogenated silicon surfaces have been produced using gas phase reactions of H-terminated Si with molecular chlorine or bromine at RT<sup>91</sup>.

Bromo-terminated Si surfaces can be obtained by treating the H-terminated Si surface with CCl<sub>3</sub>Br at 80 °C under UV irradiation. Bromination of Si-H surface is also performed sometime using an etching mixture made of F<sub>2</sub>, HNO<sub>3</sub>, CH<sub>3</sub>CO<sub>2</sub>H, Br<sub>2</sub> and KBr<sup>92</sup>, but this method causes morphology changes of Si surface<sup>93</sup>.

Iodine<sup>94,95</sup> or iodoform<sup>96</sup> have been used as iodinating agents to transform H-terminated into I-terminated Si surfaces.

Interestingly, it has not been possible to replace hydrogen by fluorine, mostly because etching in fluorinated liquids leads to H-termination<sup>97</sup> and because gas-phase fluorine (or XeF) is very aggressive, inducing strong etching.<sup>98</sup> This difficulty in obtaining F-terminated Si surfaces has motivated the work described in section 3.3, where a very recent method for partial F-termination of H-terminated Si surfaces is presented.

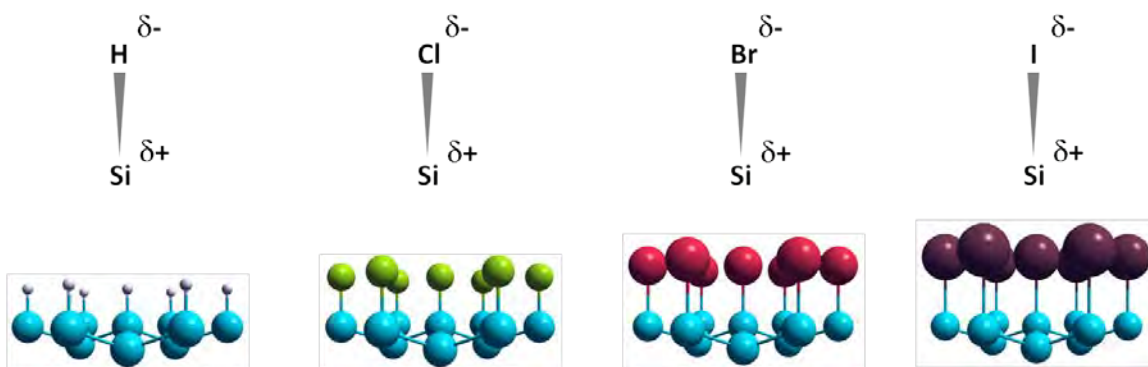


Figure 7: From left to right: H-termination, Cl-termination, Br-termination and I-termination of Si(111). Si: blue, H: white, Cl: yellow, Br: red, I: purple.

#### 3.2.2. Amino-termination

Amines are ubiquitous in biology.<sup>99</sup> Protonated amino groups (-NH<sub>3</sub><sup>+</sup>) are the most common positively charged moieties in proteins, specifically in the amino acid lysine. The anionic

polymer DNA is typically bound to various amine-rich proteins. Additionally, the terminal charged primary ammonium on lysine forms salt bridges with carboxylate groups of other amino acids in polypeptides, which is one of the primary factors of the three-dimensional structures in proteins.

There has recently been some progress made in obtaining amino functionality based on the reactions of ammonia with a clean Si surface in UHV environments. For example, ammonia reaction with clean Si(100)-2x1 surfaces has been shown experimentally and theoretically to produce Si-NH<sub>2</sub> and Si-H species in UHV conditions at RT.<sup>100-111</sup> Upon annealing to 230 °C, Si-NH<sub>2</sub> species start decomposing, resulting in the insertion of N atom to the neighboring Si-Si dimer and the formation of (Si)<sub>2</sub>=N-H. However, the clean Si(100)-2x1 surface appears unstable (i.e. suffers oxidation) outside UHV conditions. So far the ability to prepare oxygen- and carbon-free Si surfaces uniformly terminated with -NH<sub>x</sub> functionalities by wet chemistry methods has remained elusive.

On the other hand, high quality H-terminated Si surfaces can be prepared by wet chemistry methods and are stable for some time under ambient conditions. Recent detailed vibrational and mechanistic computational studies by Dai et al. indicated that H-terminated Si(111) surfaces can react with gas-phase ammonia<sup>112</sup>. The thermal reaction becomes rather complex at elevated temperatures due to N insertion into Si-Si bonds. This reaction was shown to depend on surface morphology, with ammonia reacting first with steps then atomically flat H-Si(111) terraces. Exposing H-terminated Si(111) surfaces to gas phase ammonia led to the formation of Si-NH<sub>2</sub> at first at 350°C, then with temperature increasing to 400°C the N atom inserted into Si-Si framework to produce a (N<sub>x</sub>)Si-NH<sub>y</sub> layer.

Recently, Tian et al. suggested that immersion of Cl-terminated Si surfaces in an ammonia-saturated THF solution at RT leads to amine attachment on Cl-terminated surfaces. This work raises interesting questions on the nature (NH vs. NH<sub>2</sub>) and structure (Si-NH<sub>x</sub> vs. Si-NH-Si) of the bonded NH<sub>x</sub> species.<sup>113,114</sup>

We note however that experimental evidence for amine termination of Cl/Si surfaces in NH<sub>3</sub> vapor has been questioned by Lange et al.<sup>115</sup>. Total-energy calculations show that the primary amine formation as suggested by Finstad et al.<sup>116</sup> is endothermic. Interestingly, the formation of an ionic complex at the surface was found to be more stable than the desorption of HCl (see figure 8).

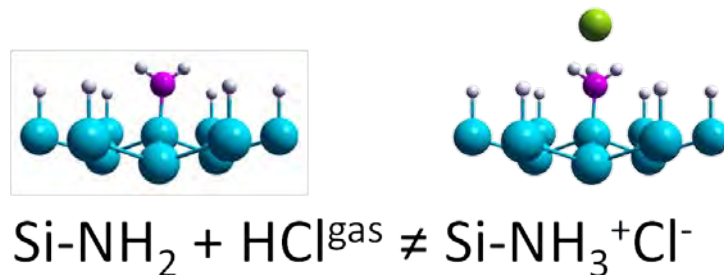


Figure 8: The primary amine (left hand) appears to be less stable than an ionic complex of the amine and HCl at the surface (right hand). Si: blue, H: white, N: purple, Cl: yellow.

### 3.3. Nanopatterning of Si(111) as a selective surface-chemistry route

#### 3.3.1. Grafting 1/3 ML methoxy on H/Si

The ability to nanopattern H-terminated Si(111) surfaces is based on the observation that immersion of H-terminated Si surfaces in alcohols leads to the attachment of alkoxy groups as replacement of hydrogen, such as methoxy for methanol, linked by Si–O–C bonds. The reaction can be thermally<sup>117,118</sup> or photochemically induced<sup>96,119</sup>, but has also been observed to take place at room temperature after long immersion times (2–3 days), clearly ruling out the need for radical formation.<sup>120</sup> In general, the preparation of monolayers linked via Si–O–C bonds to Si surfaces has typically been achieved under mild conditions, although the reaction is never complete (i.e. not all hydrogen atoms are removed) and is often associated with some partial oxidation (from remnant water molecule impurities in solution).

As recently suggested by Shirahata using contact angle measurements<sup>119</sup>, even long-chain alcohols can be grafted at 40°C, conditions under which alkenes cannot be attached. The use of such mild conditions ensures that the functional groups of the grafted molecules remain intact.<sup>121</sup> Alternatively, Zhu developed a two-step method to graft long-chain alcohols at 70°C, involving an intermediate Si–Cl surface<sup>89</sup>, and extended this approach to attach polyethylene glycol species.<sup>122</sup>

In most of these studies performed over the last decade, there is typically a small amount of interface oxide generated during the reaction as revealed by XPS or FT-IR spectroscopic studies.<sup>89,96,123</sup> Furthermore, AFM investigations have also shown that pitting occurs on initially flat H-terminated Si(111) surfaces during the grafting of alcohol species in addition to some partial oxidation.<sup>117,124</sup> In some cases, however, the grafting is achieved without oxidation. For instance, a high quality monolayer of 1-decanol has been successfully grafted on Si(111) without any detectable SiO<sub>2</sub> at the interface.<sup>121,125</sup>

In general, the observation of these two types of defects, oxidation and pitting, has undermined the interest of grafting alcohols on Si surfaces. Pitting can be partially understood by invoking mechanisms proposed to address thermal grafting on porous Si points, such as Si–Si bond breaking during reaction with alcohols with subsequent etching of Si.<sup>126</sup> Oxidation, on the other hand, is most likely caused by trace amounts of water in the alcohol solution, due to the high affinity of water for the OH group of alcohols (which is not the case for alkene molecules, for instance).

To reduce the concentration of unwanted water, Boukherroub et al. suggested adding chlorotrimethylsilane to the reaction mixture to scavenge undesirable nucleophiles during wet chemical modification of Si(111)–H.<sup>117</sup> The use of highly anhydrous chemicals was also attempted, but until recently, some oxidation of the Si could not be avoided during methanol reaction with H-terminated Si surfaces, even though the majority of the surface could clearly be perfectly methoxylated.<sup>120,126-128</sup>

The recent finding that immersion of H-terminated Si(111) surfaces in neat anhydrous methanol at 65°C inside a nitrogen purged glove box leads to the formation of oxide-free methoxy-terminated surfaces<sup>18,19</sup> confirms the role of traces of water in oxidizing the surface during alcohol reactions and highlights the importance of moderately elevated temperatures to reduce such water contamination. Processing at this temperature also brings an unexpected result, namely, that only 1/3 of a monolayer can be reacted, the other 2/3 of the surface remaining H-

terminated. The resulting surface is nanopatterned, i.e. composed of methoxy centers surrounded by six surface Si-H (see figure 9).

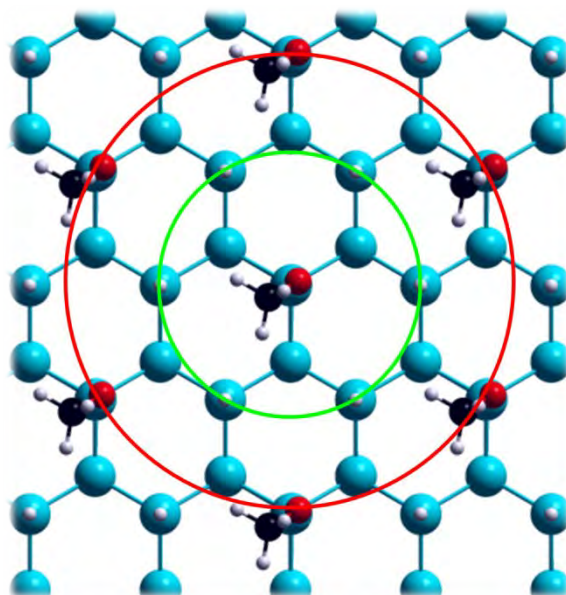


Figure 9: Top-view of the Si(111) surface with a periodic coverage of 1/3 ML methoxy- and 2/3 ML H-termination. In the structure of the nanopattern, every methoxy group is surrounded by six Si-H groups (green ring) standing as nearest neighbors (NN) and six methoxy groups (red ring) standing as next nearest neighbors (NNN). Si: blue, H: white, C: black, O: red.

The fact that the surface remains atomically flat and oxide-free after methoxylation provides a very special template for subsequent chemical reactions. It is therefore important to understand how and why this nanostructure is formed. Indeed, even if the reaction of next nearest neighbors (NNNs) is preferred, random nucleation would lead to a more disordered pattern due to a high concentration of grain boundaries between locally nanopatterned domains. That is, why the existence of a nanopattern containing precisely 1/3 ML methoxy and 2/3 ML H-termination with all methoxy groups as NNN can so far not be explained if only thermodynamics is taken into account.

Part of the understanding comes from statistical analyses of the system, and part from the fact that the process is dynamic, i.e. there is both chemisorption and removal of methoxy during the grafting process (figure 10).<sup>129</sup> Critical to this analysis is the realization that methanol decomposes at elevated temperatures with associated production of hydrogen gas. The concentration of this gas becomes an important element for surface reaction and need to be included in the calculations. If one assumes a flat, i.e., stoichiometric, H/Si(111):(1x1) surface in the presence of methanol and hydrogen, the grand canonical potential depends on both the chemical potential (concentration) of methanol and the chemical potential of hydrogen. Figure 11 shows the resulting phase diagrams of the thermodynamically stable OCH<sub>3</sub>-terminated Si(111) surface configurations after the reaction of methanol with the H-terminated Si as a function of methanol and hydrogen chemical potentials (concentrations) calculated at T = 65 °C, respectively. At that temperature, several phases are thermodynamically favorable, each

depending on both the chemical potential of methanol and the chemical potential of hydrogen as illustrated in figure 11.

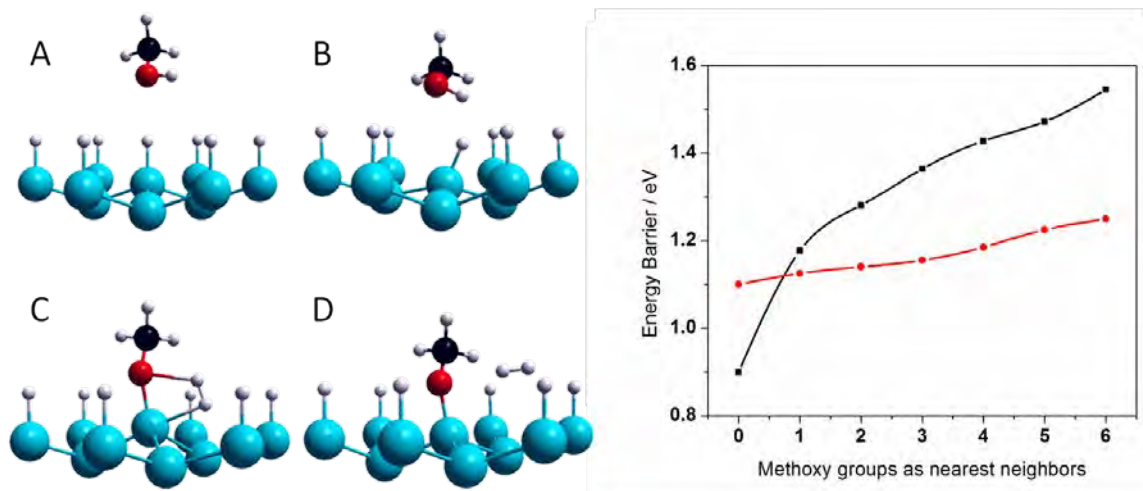


Figure 10: Left hand: Reaction mechanisms for adsorption and desorption. Methanol or hydrogen molecule attaches, interacts and is attached while the other one leaves the surface. Right hand: Calculated energy barriers of the adsorption / desorption reaction of methanol with the H-terminated Si(111) surface as a function of the number of methoxy groups as NN. Si: blue, H: white, C: black, O: red.

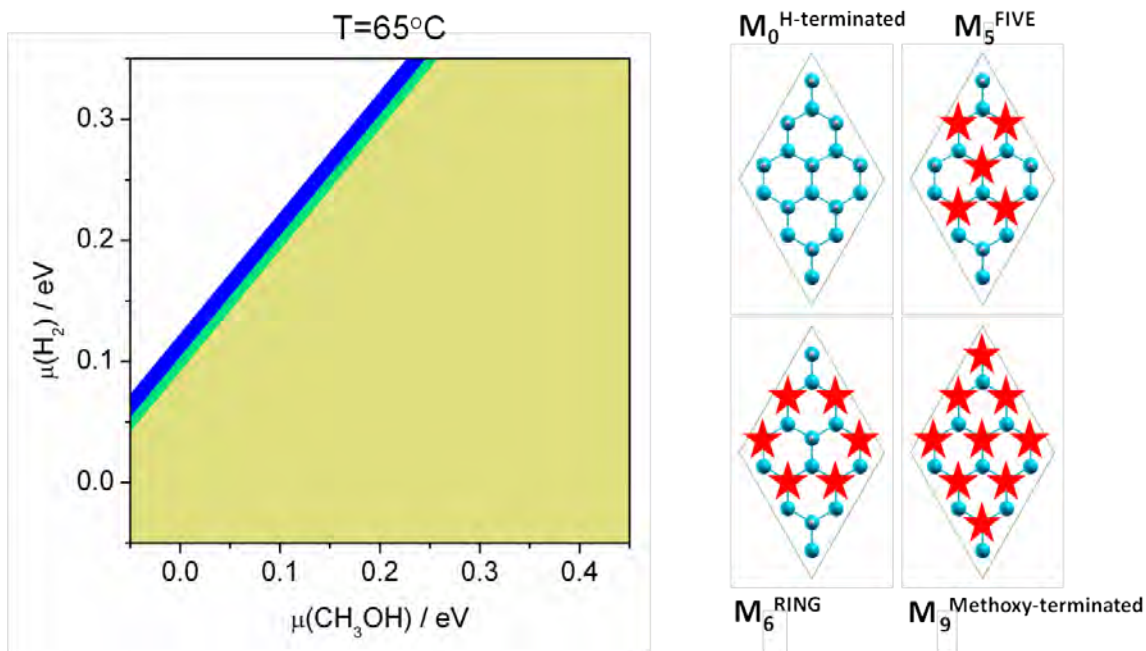


Figure 11: Left hand: Phase diagram of the thermodynamically stable Si(111) surface configurations after the reaction of methanol with the H-terminated Si(111) as a function of the methanol and hydrogen chemical potentials calculated at  $T =$

65 °C, respectively. Each color represents one of the configurations shown on the right hand side: white for the H-terminated Si(111) surface; blue for the five methoxy groups arranged as a five on a dice; green for the six methoxy groups arranged as a ring; yellow for the fully methoxy-terminated Si(111) surface. The configurations are presented as top views on the unit cell of the H-terminated Si(111) surface with red stars representing the position of methoxy groups.

H-terminated Si(111) surfaces can be reacted with methanol in a temperature-window between ~ 60-120°C. The lower T-limit is dictated by the kinetic reaction barrier, the upper limit given by the decomposition temperature of methanol. Within this temperature range, a coverage between 1/3 ML and 2/3 ML can be achieved, with 1/3 ML established at ~60°C and 2/3 ML at 120°C. Importantly within this range, the H<sub>2</sub> concentration increases with temperature, thus enhancing the back reaction and leading to a dynamic adsorption and desorption mechanism. The observation of a higher methoxy coverage at high temperatures (e.g. 2/3 ML at 120°C) suggests that it is not the thermodynamic ground state but the kinetic ground state that controls the surface coverage, and the ultimate arrangement at the surface. Since desorption of NN methoxy is enhanced and reaction of NNN sites is favored, the surface can self-organize itself into a nanopattern as observed.<sup>129</sup>

### 3.3.1. Activating this nanopatterned, oxide-free surface

Immersion of such a 1/3 methoxylated and 2/3 H-terminated surface in HF produces a F-terminated surface (see figure 12), in a way that each methoxy group is replaced by fluorine, with no changes in the surrounding Si–H groups and no attack of Si–Si bonds (i.e., no pitting). The surface remains atomically flat.<sup>19</sup>

Once F-terminated, the surface can be OH-terminated by simple immersion in water (see figure 12). Again, only the Si–F bonds are attacked, not the surrounding Si–H groups or the Si–Si back-bonds. The process can be repeated multiple times, resulting in F-termination after immersion in HF and OH-termination after immersion in water, without affecting the 2/3 ML H-termination.<sup>19</sup>

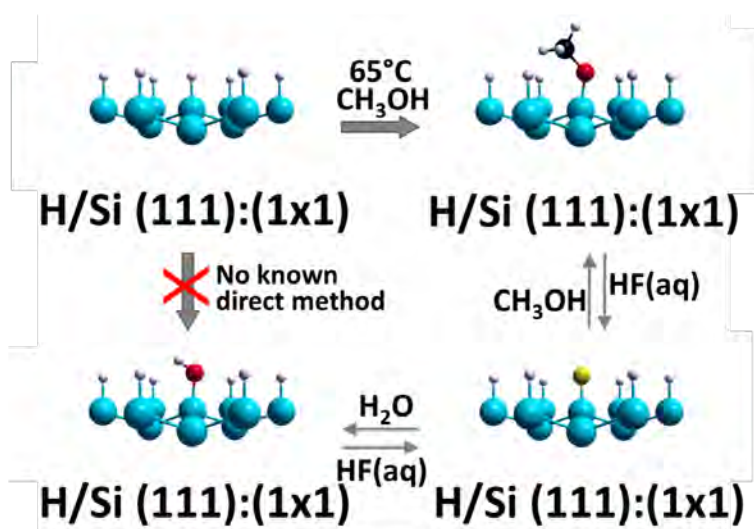


Figure 12: Overview of the chemical reactions described above. From an

atomically smooth H-terminated surface (upper left), a partial coverage of methoxy groups can be made (upper right), which serves as a nano-template for further snap chemistry to form Si-F (lower right), Si-OH (lower left) or Si-OR groups. Si: blue, H: white, C: black, O: red, F: yellow.

The formation of a partially hydroxylated surface on an otherwise oxide-free surface opens up a host of possibilities, in particular for atomic layer deposition of high and low  $\kappa$  dielectrics. For instance, HfO<sub>2</sub> and dimethyl-SiH have thus been deposited on oxide-free Si surfaces.<sup>19</sup>

In general, the presence of isolated OH groups on an otherwise hydrophobic (H-terminated) surface is of great value to attach molecules that usually could only be grafted to oxidized surfaces in the past, which is of interest for silicon-based biosensors, for instance.

### 3.4. Reactions on activated oxide-free Si(111) surfaces

#### 3.4.1. Phosphonation

Activation remains difficult for some important molecules such as phosphonic acids, and therefore constitutes a roadblock for the development of a large variety of important industrial processes and devices.<sup>130,131</sup> Among the different molecules used for SiO<sub>2</sub> chemisorption, silanes are the most popular and usually form a well-defined, densely packed SAM at RT but are highly reactive with water and with themselves, in particular in the case of trichlorosilanes, and require therefore careful handling.<sup>132,133</sup> Unlike silanes, phosphonic acids do not suffer from homocondensation and can attach to oxide surfaces initially weakly through hydrogen bonding (well-ordered physisorbed layer), and then chemically as monodentate, bidentate, tridentate, or a mixture of these configurations.<sup>130,134-142</sup>

In general, hydrogen bonding, and to a lesser extent the oxidation state of the surface Si atom, stabilize OH-terminated SiO<sub>2</sub> surfaces, and increase the reaction barrier, rendering them unfavorable for phosphonic acid chemisorption. The use of 1/3 ML OH nanopatterned Si(111) surfaces has provided insight into the nature of surface OH groups by showing that removing H-bonding and reducing the Si oxidation states leads to a fast reaction of phosphonic acid molecules on oxide-free Si at RT. Furthermore, the large distance between the OH groups forces in this case a mono-dentate configuration (see figure 13, left hand), which has important implications for the stability of the surface, as discussed next.<sup>143</sup>

Indeed, in this mono-dentate configuration, water molecules can be trapped between phosphonic acid molecules at the 1/3 ML MPA and 2/3 ML H-terminated Si(111) interface (see figure 13, right hand). The presence of these water molecules, locked in by H-bonding to P-OH and P=O, prevents other water molecules from hydrolyzing the Si-O-P bond. Interestingly, these water molecules do not affect the electronic quality of the Si/SAM interface. In comparison to purely H-terminated Si(111) surfaces, the 1/3 ML MPA, 2/3 ML H-terminated Si(111) surfaces maintain their PL yield for long times (>> 5 hours). In general, the stability of long chain SAMs has been understood in the past by the reduction of the interface ion transport. In this case, the incorporation and locking of water molecules at the interface leads to stability in aqueous solutions, representing a new mechanism for the stability of phosphonic acids grafted on Si. Thus, this model surface has made it possible to derive a detailed bonding structure and properties of phosphonic acids on Si and can be used as guide for characterization in future work and for a host of applications.

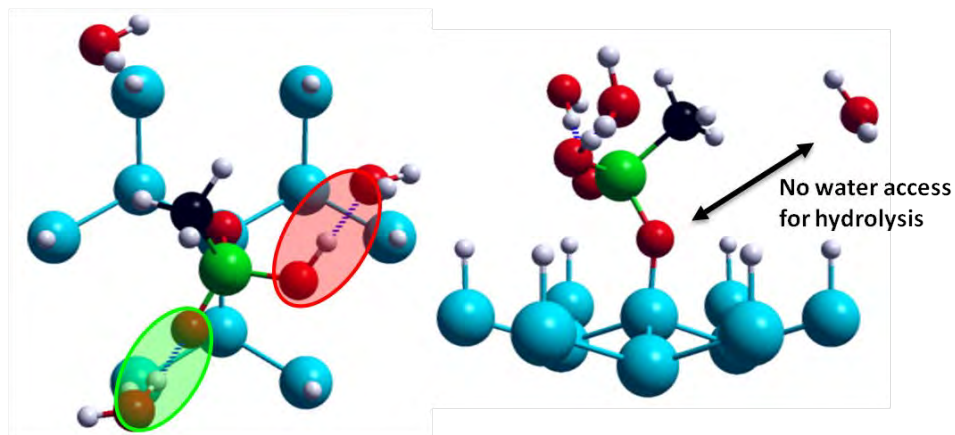


Figure 13: Location of water molecules in 1/3 ML MPA and 2/3 ML H-terminated Si(111) surface. Top and side view of 1/3 ML MPA and 2/3 ML H-terminated Si(111) surface with position of water molecules calculated to be in bridge positions. Si: blue, H: white, C: black, O: red, P: green.

### 3.4.2. Metal-hydroxides

Phosphonic acids readily attach in a variety of configurations to metal and metal oxide substrates such as magnesium,<sup>144,145</sup> aluminum,<sup>135-141,146,147</sup> silicon,<sup>5,10,130,139,143,148-150</sup> titanium,<sup>130,133,134,151-156</sup> zirconium,<sup>151,154</sup> hafnium, iron, nickel, zinc,<sup>142,157,158</sup> copper, silver, and gold,<sup>133,159</sup> and to III-V semiconductors like GaAs, InP and also light metal alloys such as AZ31.<sup>160</sup>

Attachment of the acids to surfaces takes place through a condensation reaction with surface OH groups<sup>150,161</sup> and has been shown to be more reactive towards OH groups on metal oxide than on SiO<sub>2</sub> surfaces.<sup>162,163</sup> Furthermore, phosphonic acid monolayers attached to SiO<sub>2</sub> surfaces suffer from interface-water instability, which hinders their use and applications based on SiO<sub>2</sub> surfaces.<sup>130,144,149,151</sup> In contrast, the facile grafting of phosphonic acid SAMs on aluminum oxide and the outstanding stability of their interface have been demonstrated.<sup>138,139,142,146,164</sup>

Recent findings suggest that the local atomic structure of the aluminum oxide surface is important for the stability of phosphonic acid SAMs in water, with three parameters dominating the process: i) the interfacial bonding type, ii) the adsorption free energy in the presence of water, and iii) the local atomic geometry. Consequently, the geometry of aluminum oxide surfaces needs to be taken into account.

Combining these ideas, it was recently shown that metal salts could be used to conformally coat SiO<sub>2</sub> surfaces with the goal of enhancing the bonding and stability of phosphonic acid SAMs. Such thin coatings of metal oxides had previously been prepared by vapor phase methods such as ALD. The use of solution phase chemistry based on aqueous salt solutions makes the method simpler and more applicable for many applications. The wet chemical approach is all the more attractive that the deposition was shown to be controllable down to the submonolayer level. Furthermore, facile grafting of phosphonic acid molecules was demonstrated, with good stability

in aqueous solutions.

Molecular binding of ODPA to a surface appears to be highly dependent on the distance between the phosphorus atom and the underlying metal ion. Hector et al.<sup>165</sup> established in 2001 for instance, in a first-principles study, that the distance between the phosphorous in the phosphonic acid head group and the underlying aluminum ion is a crucial parameter controlling the stability of the binding geometry. By studying different binding geometries of vinylphosphonic acid on  $\text{Al}_2\text{O}_3(0001)$ , they found the tridentate model most stable because it has the largest distance between P and Al, compared to the other model geometries.

Figure 14 depicts for instance all possible triangular adsorption sites on the fully hydroxylated  $\text{Al}_2\text{O}_3(0001)$  surface, which correspond to the thermodynamic ground states of aluminum oxide in water.<sup>163</sup> The tridentate adsorption of phosphonic acids is only possible on the adsorption sites A and B, mostly because of their distance to the underlying metal ion. On the adsorption sites C and D, the bidentate is the thermodynamic ground state. The tridentate phosphonates have the shortest P--Al distance in comparison to bi- and mono-dentates, and thus the highest repulsive interaction.<sup>166</sup>

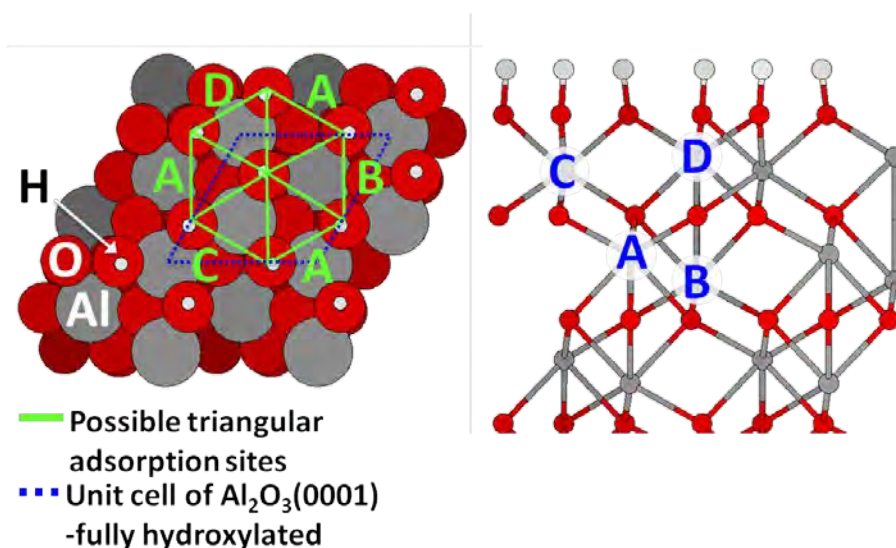


Figure 14: Fully hydroxylated  $\text{Al}_2\text{O}_3(0001)$  surface with all possible triangular adsorption sites.

In order to gain a more detailed understanding of phosphonate bonding at surfaces, use of the model surface was made by treating the 1/3 ML OH-terminated surface guided by the newly developed wet chemical approach (i.e.  $\sim 1$  min in a  $\text{AlCl}_3$  salt solution). On this surface, every Si-OH group is grafted with  $\text{Al}(\text{OH})_3$  to form *isolated* Si-O-Al(OH)<sub>2</sub> units, i.e. separated by 3.9 Å which is too far to present a dense matrix for phosphonic acid adsorption. Again, the model surface is ideal to explore the bonding of a phosphonic acid molecule on a *single* Al atom.

Starting from the lowest energy adsorption configuration of a 1/3 ML Al-(OH)<sub>2</sub> and 2/3 ML H-terminated Si(111) on the H/Si(111):(1x1) surface unit cell, the reaction pathway of a heterocondensation was examined theoretically, as illustrated in figure 15. The corresponding

lowest energy structures obtained from various starting geometries for the respective coverage on the surface are shown in figure 15, including the physisorption state (left), the intermediate monodentate state (middle) and the final bidentate state (right). Importantly, the tridentate state of phosphonic acids is found not to be stable on the 1/3 ML Al-(OH)<sub>2</sub> and 2/3 ML H-terminated Si(111) model surface. The main reason is the short distance to the underlying metal ion leading to strong repulsive interactions. This distance is decreasing from 4.8 Å ( physisorbed), to 3.0 Å ( monodentate), to 2.5 Å ( bidentate).

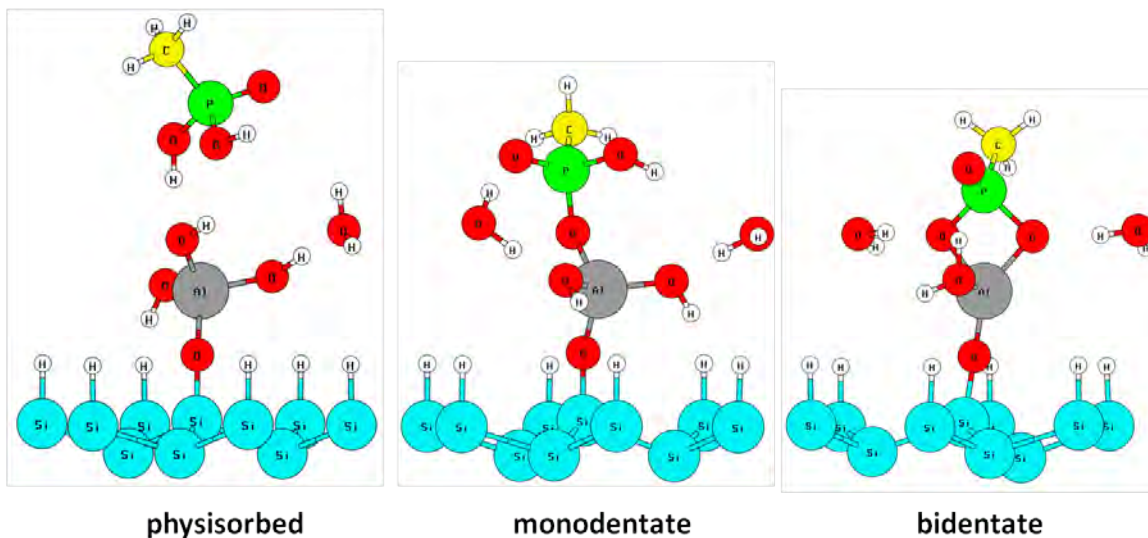


Figure 15: Calculated configurations obtained as MPA is approaching an isolated Si-O-Al(OH)<sub>2</sub>. Note that two water molecules are eliminated during this heterocondensation reaction.

The tridentate adsorption can therefore only be achieved if two distinct Al atoms are involved, as described in detail in the case of the Al<sub>2</sub>O<sub>3</sub>(0001) surface (figure 14). The model surface has therefore made it possible to gain unprecedented insight into the fundamentals of phosphonate adsorption.<sup>167</sup>

With this knowledge, the wet chemical method presented above can help bring phosphonic acids into industrial applications. This is important as phosphonic acids are promising for manufacturing ultralow voltage organic TFT on delicate substrates, such as banknotes.<sup>168,169</sup>

#### 4. Concluding remarks and outlook

In this review, a case was made for functionalizing oxide-free Si surfaces. Indirect and direct substitution methods were described and briefly summarized. More emphasis was placed on direct substitution by methanol as a starting point because of the formation of a nanopatterned surface on atomically flat Si(111) surfaces.

This interesting chemically patterned surface was shown to be easily functionalized, making it possible to explore surface chemistry in some detail. As an example, phosphonation of oxide-free surfaces with isolated OH groups was described both on the OH groups and after metal oxide modification of the OH groups with metal salts. It was shown in particular that the

fundamentals of phosphonate adsorption could be unraveled by understanding and controlling the formation of mono-, bi- and tri-dentate adsorption.

Overall, this work presents a platform for further investigations into two fruitful directions. First, the direct modification of H/Si surfaces with alcohols should be pursued by considering i) other Si faces, notably Si(100) that displays a very interesting nanostructure and ii) longer chain alcohols or acids to determine whether and what type of chemical nanostructuring can also be achieved. Second, the functionalization of isolated OH groups with metals other than aluminum should be explored by determining the conditions (notably pH) for grafting other metals. Recent experiments, for instance, have shown that magnesium oxide cannot adsorb onto SiO<sub>2</sub> surfaces in neutral or acidic solutions. However, in a basic pH solution, the magnesium ion coordinates with hydroxide ions and the thermodynamics of this complex favors deposition and crystallization.

Metallic transformation of OH-terminated surfaces is promising because a variety of metals is used in alloy manufacturing. The most common are iron, aluminum, magnesium, zinc, manganese, copper, chromium, nickel and molybdenum. An interesting question will be if any other metals or alloys could reduce the repulsive interaction of phosphonic acids to the underlying metal ion. Beyond the grafting of phosphonates, other metals may also foster grafting of other groups like carboxylates and silanes.

In general, the attachment of organic molecules can be optimized by selection of the proper metal oxide. Therefore, control of metal oxide composition and coverage may be particularly useful for complex applications. For example, MOFs are difficult to grow epitaxially on any substrate, despite their fascinating properties and many potential applications like chemical sensors, filters, gas storage, smart membranes<sup>170</sup>. Up to now, there are three known wet chemical methods to fabricate so called surface MOFs, or SURMOFs: (1) direct deposition from mother solution, (2) assembly of preformed, size- and shape-selected nanocrystals and (3) stepwise LBL deposition.<sup>171-174</sup> The controlled deposition of low coverage and well-structured metals on silicon, combined with tunable chemical functionality, will therefore play a key-role in the epitaxial growth of MOFs.

## **5. Acknowledgements**

This work was mainly supported by the National Science Foundation (Grant CHE-0911197) and partly by the Texas Higher Education Coordinating Board (NHAR Program). P. Thissen acknowledges the partial support by the Deutsche Forschungsgemeinschaft (DFG).

## 6. References

- (1) Helms, C. R.; Poindexter, E. H. *Reports on Progress in Physics* **1994**, *57*, 791-852.
- (2) Sze, S. M. *Physics of semiconductor devices*; Wiley-Interscience: New-York, 1981; Vol. 2.
- (3) Miller, J. B.; Schwartz, J.; Bernasek, S. L. *Journal of the American Chemical Society* **1993**, *115*, 8239-8247.
- (4) Rye, R. R.; Nelson, G. C.; Dugger, M. T. *Langmuir* **1997**, *13*, 2965-2972.
- (5) Hanson, E. L.; Schwartz, J.; Nickel, B.; Koch, N.; Danisman, M. F. *Journal of the American Chemical Society* **2003**, *125*, 16074-16080.
- (6) Rozlosnik, N.; Gerstenberg, M. C.; Larsen, N. B. *Langmuir* **2003**, *19*, 1182-1188.
- (7) Wang, Y. L.; Lieberman, M. *Langmuir* **2003**, *19*, 1159-1167.
- (8) Vega, A.; Thissen, P.; Chabal, Y. J. *Langmuir* **2012**.
- (9) Higashi, G. S.; Chabal, Y. J.; Trucks, G. W.; Raghavachari, K. *Applied Physics Letters* **1990**, *56*, 656-658.
- (10) Buriak, J. M. *Chemical Reviews* **2002**, *102*, 1271-1308.
- (11) Cicero, R. L.; Linfood, M. R.; Chidsey, C. E. D. *Langmuir* **2000**, *16*, 5688-5695.
- (12) Linfood, M. R.; Fenter, P.; Eisenberger, P. M.; Chidsey, C. E. D. *Journal of the American Chemical Society* **1995**, *117*, 3145-3155.
- (13) Sieval, A. B.; Linke, R.; Zuilhof, H.; Sudholter, E. J. R. *Advanced Materials* **2000**, *12*, 1457-1460.
- (14) deVilleneuve, C. H.; Pinson, J.; Bernard, M. C.; Allongue, P. *Journal of Physical Chemistry B* **1997**, *101*, 2415-2420.
- (15) Fabre, B.; Lopinski, G. P.; Wayner, D. D. M. *Chemical Communications* **2002**, 2904-2905.
- (16) Kim, N. Y.; Laibinis, P. E. *Journal of the American Chemical Society* **1999**, *121*, 7162-7163.
- (17) Bansal, A.; Li, X. L.; Lauermann, I.; Lewis, N. S.; Yi, S. I.; Weinberg, W. H. *Journal of the American Chemical Society* **1996**, *118*, 7225-7226.
- (18) Michalak, D. J.; Amy, S. R.; Esteve, A.; Chabal, Y. J. *Journal of Physical Chemistry C* **2008**, *112*, 11907-11919.
- (19) Michalak, D. J.; Amy, S. R.; Aureau, D.; Dai, M.; Esteve, A.; Chabal, Y. J. *Nature Materials* **2010**, *9*, 266-271.
- (20) Weinberger, B. R.; Deckman, H. W.; Yablonovitch, E.; Gmitter, T.; Kobasz, W.; Garoff, S. *Journal of Vacuum Science & Technology a-Vacuum Surfaces and Films* **1985**, *3*, 887-891.
- (21) Ubara, H.; Imura, T.; Hiraki, A. *Solid State Communications* **1984**, *50*, 673-675.

- (22) Chabal, Y. J.; Higashi, G. S.; Raghavachari, K.; Burrows, V. A. *Journal of Vacuum Science & Technology A: Vacuum, Surfaces, and Films* **1989**, *7*, 2104-2109.
- (23) Imura, T.; Mogi, K.; Hiraki, A.; Nakashima, S.; Mitsuishi, A. *Solid State Communications* **1981**, *40*, 161-164.
- (24) Trucks, G. W.; Raghavachari, K.; Higashi, G. S.; Chabal, Y. J. *Physical Review Letters* **1990**, *65*, 504.
- (25) Hines, M. A.; Faggin, M. F.; Gupta, A.; Aldinger, B. S.; Bao, K. *The Journal of Physical Chemistry C* **2012**, *116*, 18920-18929.
- (26) Allongue, P.; Henry de Villeneuve, C.; Morin, S.; Boukherroub, R.; Wayner, D. D. M. *Electrochimica Acta* **2000**, *45*, 4591-4598.
- (27) Faggin, M. F.; Green, S. K.; Clark, I. T.; Queeney, K. T.; Hines, M. A. *Journal of the American Chemical Society* **2006**, *128*, 11455-11462.
- (28) Clark, I. T.; Aldinger, B. S.; Gupta, A.; Hines, M. A. *The Journal of chemical physics* **2008**, *128*, 144711.
- (29) Jakob, P.; Chabal, Y. J. *The Journal of Chemical Physics* **1991**, *95*, 2897-2909.
- (30) Jakob, P.; Chabal, Y. L.; Raghavachari, K. *Chemical Physics Letters* **1991**, *187*, 325-333.
- (31) Jakob, P.; Chabal, Y. J.; Raghavachari, K.; Becker, R. S.; Becker, A. J. *Surface Science* **1992**, *275*, 407-413.
- (32) Hines, M. A. *Int. Rev. Phys. Chem.* **2001**, *20*, 645-672.
- (33) Clark, I. T.; Aldinger, B. S.; Gupta, A.; Hines, M. A. *The Journal of Physical Chemistry C* **2009**, *114*, 423-428.
- (34) Yablonovitch, E.; Allara, D. L.; Chang, C. C.; Gmitter, T.; Bright, T. B. *Physical Review Letters* **1986**, *57*, 249-252.
- (35) Zhang, X.; Garfunkel, E.; Chabal, Y. J.; Christman, S. B.; Chaban, E. E. *Applied Physics Letters* **2001**, *79*, 4051-4053.
- (36) Ye, S.; Saito, T.; Nihonyanagi, S.; Uosaki, K.; Miranda, P. B.; Kim, D.; Shen, Y. R. *Surface Science* **2001**, *476*, 121-128.
- (37) Eastman, D. E.; Chiang, T. C.; Heimann, P.; Himpsel, F. J. *Physical Review Letters* **1980**, *45*, 656-659.
- (38) Himpsel, F. J.; Heimann, P.; Chiang, T. C.; Eastman, D. E. *Physical Review Letters* **1980**, *45*, 1112-1115.
- (39) Himpsel, F. J.; Meyerson, B. S.; McFeely, F. R.; Morar, J. F.; Talebibrabimi, A.; Yarmoff, J. A. In *Photoemission and Absorption Spectroscopy of Solids and Interfaces with Synchrotron Radiation* 1990; Vol. 108, p 203-236.
- (40) Linford, M. R.; Chidsey, C. E. D. *Journal of the American Chemical Society* **1993**, *115*, 12631-12632.

- (41) Aswal, D. K.; Lenfant, S.; Guerin, D.; Yakhmi, J. V.; Vuillaume, D. *Anal. Chim. Acta* **2006**, *568*, 84-108.
- (42) Boukherroub, R. *Current Opinion in Solid State and Materials Science* **2005**, *9*, 66-72.
- (43) Shirahata, N.; Hozumi, A.; Yonezawa, T. *The Chemical Record* **2005**, *5*, 145-159.
- (44) Wayner, D. D. M.; Wolkow, R. A. *Journal of the Chemical Society- Perkin Transactions* **2002**, *2*, 23 - 34.
- (45) Aureau, D.; Chabal, Y. In *Functionalization of Semiconductor Surfaces*; Tao, F., Bernasek, S. L., Eds.; John Wiley & Sons, Inc.: New-York, 2012; Vol. 1.
- (46) Asao, N.; Sudo, T.; Yamamoto, Y. *The Journal of Organic Chemistry* **1996**, *61*, 7654-7655.
- (47) Boukherroub, R.; Morin, S.; Bensebaa, F.; Wayner, D. D. M. *Langmuir* **1999**, *15*, 3831-3835.
- (48) Chalk, A. J.; Harrod, J. F. *Journal of the American Chemical Society* **1965**, *87*, 16-21.
- (49) Marciniak, B. *Silicon Chemistry* **2002**, *1*, 155-174.
- (50) Sommer, L. H.; Pietrusza, E. W.; Whitmore, F. C. *Journal of the American Chemical Society* **1947**, *69*, 188-188.
- (51) Song, Y.-S.; Yoo, B. R.; Lee, G.-H.; Jung, I. N. *Organometallics* **1999**, *18*, 3109-3115.
- (52) Speier, J. L.; Webster, J. A.; Barnes, G. H. *Journal of the American Chemical Society* **1957**, *79*, 974-979.
- (53) Webb, L. J.; Lewis, N. S. *Journal of Physical Chemistry B* **2003**, *107*, 5404-5412.
- (54) de Smet, L. C. P. M.; Zuilhof, H.; Sudholter, E. J. R.; Lie, L. H.; Houlton, A.; Horrocks, B. R. *Journal of Physical Chemistry B* **2005**, *109*, 12020-12031.
- (55) Woods, M.; Carlsson, S.; Hong, Q.; Patole, S. N.; Lie, L. H.; Houlton, A.; Horrocks, B. R. *The Journal of Physical Chemistry B* **2005**, *109*, 24035-24045.
- (56) Arafat, S. N.; Dutta, S.; Perring, M.; Mitchell, M.; Kenis, P. J. A.; Bowden, N. B. *Chemical Communications* **2005**, 3198-3200.
- (57) Perring, M.; Dutta, S.; Arafat, S.; Mitchell, M.; Kenis, P. J. A.; Bowden, N. B. *Langmuir* **2005**, *21*, 10537-10544.
- (58) Schmeltzer, J. M.; Porter, L. A.; Stewart, M. P.; Buriak, J. M. *Langmuir* **2002**, *18*, 2971-2974.
- (59) Webb, L. J.; Rivillon, S.; Michalak, D. J.; Chabal, Y. J.; Lewis, N. S. *Journal of Physical Chemistry B* **2006**, *110*, 7349-7356.
- (60) Wang, X.; Ruther, R. E.; Streifer, J. A.; Hamers, R. J. *Journal of the American Chemical Society* **2010**, *132*, 4048-4049.

- (61) Sun, Q. Y.; deSmet, L. C. P. M.; vanLagen, B.; Giesbers, M.; Thune, P. C.; vanEngelenburg, J.; deWolf, F. A.; Zuilhof, H.; Sudholter, E. J. R. *Journal of the American Chemical Society* **2005**, *127*, 2514-2523.
- (62) ter Maat, J.; Regeling, R.; Yang, M.; Mullings, M. N.; Bent, S. F.; Zuilhof, H. *Langmuir* **2009**, *25*, 11592-11597.
- (63) Vong, T.; ter Maat, J.; van Beek, T. A.; van Lagen, B.; Giesbers, M.; van Hest, J. C. M.; Zuilhof, H. *Langmuir* **2009**, *25*, 13952-13958.
- (64) Demierry, P.; Ballutaud, D.; Aucouturier, M.; Etcheberry, A. *J. Electrochem. Soc.* **1990**, *137*, 2966-2973.
- (65) Aureau, D.; Rappich, J.; Moraillon, A.; Allongue, P.; Ozanam, F.; Chazalviel, J. N. *Journal of Electroanalytical Chemistry* **2010**, *646*, 33-42.
- (66) Sieval, A. B.; Demirel, A. L.; Nissink, J. W. M.; Linford, M. R.; van der Maas, J. H.; de Jeu, W. H.; Zuilhof, H.; Sudholter, E. J. R. *Langmuir* **1998**, *14*, 1759-1768.
- (67) Sieval, A. B.; Linke, R.; Zuilhof, H.; Sudhölter, E. J. R. *Advanced Materials* **2000**, *12*, 1457-1460.
- (68) Buriak, J. M. *Chemical Communications* **1999**, 1051-1152.
- (69) Sieval, A. B.; Opitz, R.; Maas, H. P. A.; Schoeman, M. G.; Meijer, G.; Vergeldt, F. J.; Zuilhof, H.; Sudholter, E. J. R. *Langmuir* **2000**, *16*, 10359-10368.
- (70) Mischki, T. K.; Lopinski, G. P.; Wayner, D. D. M. *Langmuir* **2009**, *25*, 5626-5630.
- (71) Boukherroub, R.; Szunerits, S. In *Electrochemistry at the nanoscale*; Schmuki, P., Virtanen, S., Eds.; Springer New York: New York, 2009, p 183-248.
- (72) Coletti, C.; Marrone, A.; Giorgi, G.; Sgamellotti, A.; Cerofolini, G.; Re, N. *Langmuir* **2006**, *22*, 9949-9956.
- (73) Ng, A.; Ciampi, S.; James, M.; Harper, J. B.; Gooding, J. J. *Langmuir* **2009**, *25*, 13934-13941.
- (74) Scheres, L.; Giesbers, M.; Zuilhof, H. *Langmuir* **2010**, *26*, 4790-4795.
- (75) Scheres, L.; Arafat, A.; Zuilhof, H. *Langmuir* **2007**, *23*, 8343-8346.
- (76) Scheres, L.; Giesbers, M.; Zuilhof, H. *Langmuir* **2010**, *26*, 10924-10929.
- (77) Seitz, O.; Dai, M.; Aguirre-Tostado, F. S.; Wallace, R. M.; Chabal, Y. J. *Journal of the American Chemical Society* **2009**, *131*, 18159-18167.
- (78) Aureau, D.; Varin, Y.; Roodenko, K.; Seitz, O.; Pluchery, O.; Chabal, Y. J. *The Journal of Physical Chemistry C* **2010**, *114*, 14180-14186.
- (79) Dietrich, P.; Michalik, F.; Schmidt, R.; Gahl, C.; Mao, G.; Breusing, M.; Raschke, M.; Priewisch, B.; Elsässer, T.; Mendelsohn, R.; Weinelt, M.; Rück-Braun, K. *Applied Physics A: Materials Science & Processing* **2008**, *93*, 285-292.
- (80) Touahir, L.; Allongue, P.; Aureau, D.; Boukherroub, R.; Chazalviel, J. N.; Galopin, E.; Gouget-Laemmel, A. C.; de Villeneuve, C. H.; Moraillon, A.; Niedziółka-Jönsson,

- J.; Ozanam, F.; Andresa, J. S.; Sam, S.; Solomon, I.; Szunerits, S. *Bioelectrochemistry* **2010**, *In Press*, *Corrected Proof*.
- (81) Chazalviel, J. N.; Allongue, P.; Gouget-Laemmel, A. C.; de Villeneuve, C. H.; Moraillon, A.; Ozanam, F. *Science of Advanced Materials*, **3**, 332-353.
- (82) Seitz, O.; Fernandes, P. G.; Mahmud, G. A.; Wen, H.-C.; Stiegler, H. J.; Chapman, R. A.; Vogel, E. M.; Chabal, Y. J. *Langmuir* **2011**, *27*, 7337-7340.
- (83) Seitz, O.; Bäcking, T.; Salomon, A.; Gooding, J. J.; Cahen, D. *Langmuir* **2006**, *22*, 6915-6922.
- (84) Magid, I.; Burstein, L.; Seitz, O.; Segev, L.; Kronik, L.; Rosenwaks, Y. *The Journal of Physical Chemistry C* **2008**, *112*, 7145-7150.
- (85) Nguyen, H. M.; Seitz, O.; Peng, W.; Gartstein, Y. N.; Chabal, Y. J.; Malko, A. V. *ACS Nano* **2012**, *6*, 5574-5582.
- (86) Seitz, O.; Caillard, L.; Nguyen, H. M.; Chiles, C.; Chabal, Y. J.; Malko, A. V. *Applied Physics Letters* **2011**, Submitted.
- (87) Peng, W.; Seitz, O.; Chapman, R. A.; Vogel, E. M.; Chabal, Y. J. *Applied Physics Letters* **2012**, *101*, 051605-5.
- (88) Bansal, A.; Li, X. L.; Yi, S. I.; Weinberg, W. H.; Lewis, N. S. *Journal of Physical Chemistry B* **2001**, *105*, 10266-10277.
- (89) Zhu, X. Y.; Boiadjev, V.; Mulder, J. A.; Hsung, R. P.; Major, R. C. *Langmuir* **2000**, *16*, 6766-6772.
- (90) Rivillon, S.; Amy, F.; Chabal, Y. J.; Frank, M. M. *Applied Physics Letters* **2004**, *85*, 2583-2585.
- (91) Eves, B. J.; Lopinski, G. P. *Surface Science* **2005**, *579*, L89-L96.
- (92) Narducci, D.; Pedemonte, L.; Bracco, G. *Applied Surface Science* **2003**, *212*, 649-653.
- (93) Pedemonte, L.; Bracco, G.; Relini, A.; Rolandi, R.; Narducci, D. *Applied Surface Science* **2003**, *212*, 595-600.
- (94) Lauerhaas, J. M.; Sailor, M. J. *Science* **1993**, *261*, 1567-1568.
- (95) Lauerhaas, J. M.; Sailor, M. J. In *Silicon-Based Optoelectronic Materials* 1993; Vol. 298, p 259-263.
- (96) Joy, V. T.; Mandler, D. *Chemphyschem* **2002**, *3*, 973-975.
- (97) Love, J. C.; Estroff, L. A.; Kriebel, J. K.; Nuzzo, R. G.; Whitesides, G. M. *Chemical Reviews* **2005**, *105*, 1103-1169.
- (98) Roth, K. M.; Dontha, N.; Dabke, R. B.; Gryko, D. T.; Clausen, C.; Lindsey, J. S.; Bocian, D. F.; Kuhr, W. G. *Journal of Vacuum Science & Technology B* **2000**, *18*, 2359-2364.
- (99) Dill, K. A. *Biochemistry* **1990**, *29*, 7133-7155.
- (100) Bowler, D. R.; Owen, J. H. G. *Physical Review B* **2007**, *75*.

- (101) Chung, O. N.; Kim, H.; Chung, S.; Koo, J. Y. *Physical Review B* **2006**, *73*.
- (102) Kim, Y.-S.; Koo, J.-Y.; Kim, H. *Physical Review Letters* **2008**, *100*.
- (103) Kim, Y.-S.; Koo, J.-Y.; Kim, H. *Journal of physics. Condensed matter : an Institute of Physics journal* **2009**, *21*, 064237-064237.
- (104) Kubler, L.; Bischoff, J. L.; Bolmont, D. *Physical Review B* **1988**, *38*, 13113-13123.
- (105) Mathieu, C.; Bai, X.; Bournel, F.; Gallet, J. J.; Carniato, S.; Rochet, F.; Sirotti, F.; Silly, M. G.; Chauvet, C.; Krizmancic, D.; Hennies, F. *Physical Review B* **2009**, *79*.
- (106) Owen, J. H. G. *Journal of Physics-Condensed Matter* **2009**, *21*.
- (107) Rangelov, G.; Stober, J.; Eisenhut, B.; Fauster, T. *Physical Review B* **1991**, *44*, 1954-1957.
- (108) Rodriguez-Reyes, J. C. F.; Teplyakov, A. V. *Physical Review B* **2007**, *76*.
- (109) Rodriguez-Reyes, J. C. F.; Teplyakov, A. V. *Physical Review B* **2008**, *78*.
- (110) Widjaja, Y.; Musgrave, C. B. *Surface Science* **2000**, *469*, 9-20.
- (111) Widjaja, Y.; Mysinger, M. M.; Musgrave, C. B. *Journal of Physical Chemistry B* **2000**, *104*, 2527-2533.
- (112) Dai, M.; Wang, Y.; Kwon, J.; Halls, M. D.; Chabal, Y. J. *Nature Materials* **2009**, *8*, 825-830.
- (113) Tian, F.; Taber, D. F.; Teplyakov, A. V. *Journal of the American Chemical Society*, *133*, 20769-20777.
- (114) Tian, F.; Yang, D.; Opila, R. L.; Teplyakov, A. V. *Applied Surface Science*, *258*, 3019-3026.
- (115) Lange, B.; Schmidt, W. G. *Surface Science* **2008**, *602*, 1207-1211.
- (116) Finstad, C. C.; Thorsness, A. G.; Muscat, A. J. *Surface Science* **2006**, *600*, 3363-3374.
- (117) Boukherroub, R.; Morin, S.; Sharpe, P.; Wayner, D. D. M.; Allongue, P. *Langmuir* **2000**, *16*, 7429-7434.
- (118) Cleland, G.; Horrocks, B. R.; Houlton, A. *Journal of the Chemical Society-Faraday Transactions* **1995**, *91*, 4001-4003.
- (119) Hozumi, A.; Taoda, H.; Saito, T.; Shirahata, N. *Journal of Nanoscience and Nanotechnology* **2009**, *9*, 455-460.
- (120) Michalak, D. J.; Rivillon, S.; Chabal, Y. J.; Esteve, A.; Lewis, N. S. *Journal of Physical Chemistry B* **2006**, *110*, 20426-20434.
- (121) Thieblemont, F.; Seitz, O.; Vilan, A.; Cohen, H.; Salomon, E.; Kahn, A.; Cahen, D. *Advanced Materials* **2008**, *20*, 3931-+.
- (122) Zhu, X. Y.; Jun, Y.; Staarup, D. R.; Major, R. C.; Danielson, S.; Boiadjev, V.; Gladfelter, W. L.; Bunker, B. C.; Guo, A. *Langmuir* **2001**, *17*, 7798-7803.

- (123) Saito, N.; Lee, S. H.; Maeda, N.; Ohta, R.; Sugimura, H.; Takai, O. *Journal of Vacuum Science & Technology A* **2004**, *22*, 1425-1427.
- (124) Dusciac, D.; Chazalviel, J.-N.; Ozanam, F.; Allongue, P.; de Villeneuve, C. H. *Surface Science* **2007**, *601*, 3961-3964.
- (125) Wallart, X.; de Villeneuve, C. H.; Allongue, P. *Journal of the American Chemical Society* **2005**, *127*, 7871-7878.
- (126) Bateman, J. E.; Horrocks, B. R.; Houlton, A. *Journal of the Chemical Society-Faraday Transactions* **1997**, *93*, 2427-2431.
- (127) Haber, J. A.; Lauermann, I.; Michalak, D.; Vaid, T. P.; Lewis, N. S. *Journal of Physical Chemistry B* **2000**, *104*, 9947-9950.
- (128) Hory, M. A.; Herino, R.; Ligeon, M.; Muller, F.; Gaspard, F.; Mihalcescu, I.; Vial, J. C. *Thin Solid Films* **1995**, *255*, 200-203.
- (129) Thissen, P.; Roodenko, K.; Fuchs, E.; Peixoto, T.; Batchelor, B., Smith, D., Schmidt, W. G.; Chabal, Y. J., *Journal of the American Chemical Society*, submitted **2012**.
- (130) Mutin, P. H.; Lafond, V.; Popa, A. F.; Granier, M.; Markey, L.; Dereux, A. *Chemistry of Materials* **2004**, *16*, 5670-5675.
- (131) Raman, A.; Quinones, R.; Barriger, L.; Eastman, R.; Parsi, A.; Gawalt, E. S. *Langmuir* **2010**, *26*, 1747-1754.
- (132) Vandervoort, P.; Gillisdhamers, I.; Vansant, E. F. *Journal of the Chemical Society-Faraday Transactions* **1990**, *86*, 3751-3755.
- (133) Mani, G.; Johnson, D. M.; Marton, D.; Dougherty, V. L.; Feldman, M. D.; Patel, D.; Ayon, A. A.; Agrawal, C. M. *Langmuir* **2008**, *24*, 6774-6784.
- (134) Luschtinetz, R.; Frenzel, J.; Milek, T.; Seifert, G. *Journal of Physical Chemistry C* **2009**, *113*, 5730-5740.
- (135) Luschtinetz, R.; Oliveira, A. F.; Duarte, H. A.; Seifert, G. *Zeitschrift Fur Anorganische Und Allgemeine Chemie* **2010**, *636*, 1506-1512.
- (136) Luschtinetz, R.; Oliveira, A. F.; Frenzel, J.; Joswig, J.-O.; Seifert, G.; Duarte, H. A. *Surface Science* **2008**, *602*, 1347-1359.
- (137) Luschtinetz, R.; Seifert, G.; Jaehne, E.; Adler, H. J. P. *Macromolecular Symposia* **2007**, *254*, 248-253.
- (138) Lassiaz, S.; Galarneau, A.; Trens, P.; Labarre, D.; Mutin, H.; Brunel, D. *New Journal of Chemistry* **2010**, *34*, 1424-1435.
- (139) Lassiaz, S.; Labarre, D.; Galarneau, A.; Brunel, D.; Mutin, P. H. *Journal of Materials Chemistry* **2011**, *21*, 8199-8205.
- (140) Maege, I.; Jaehne, E.; Henke, A.; Adler, H.-J. P.; Bram, C.; Jung, C.; Stratmann, M. *Progress in Organic Coatings* **1997**, *34*, 1-12.
- (141) Thissen, P.; Valtiner, M.; Grundmeier, G. *Langmuir* **2010**, *26*, 156-164.

- (142) Thissen, P.; Wielant, J.; Koeyer, M.; Toews, S.; Grundmeier, G. *Surface & Coatings Technology* **2010**, *204*, 3578-3584.
- (143) Thissen, P.; Peixoto, T.; Longo, R. C.; Peng, W.; Schmidt, W. G.; Cho, K.; Chabal, Y. J. *Journal of the American Chemical Society* **2012**, *134*, 8869-8874.
- (144) Mutin, P. H.; Guerrero, G.; Vioux, A. *Comptes Rendus Chimie* **2003**, *6*, 1153-1164.
- (145) Thissen, P.; Thissen, V.; Wippermann, S.; Chabal, Y. J.; Grundmeier, G.; Schmidt, W. G. *Surface Science* **2012**, *606*, 902-907.
- (146) Maxisch, M.; Thissen, P.; Giza, M.; Grundmeier, G. *Langmuir* **2011**, *27*, 6042-6048.
- (147) Wapner, K.; Stratmann, M.; Grundmeier, G. *International Journal of Adhesion and Adhesives* **2008**, *28*, 59-70.
- (148) Acton, O.; Hutchins, D.; Arnadottir, L.; Weidner, T.; Cernetic, N.; Ting, G. G.; Kim, T. W.; Castner, D. G.; Ma, H.; Jen, A. K. Y. *Advanced Materials* **2011**, *23*, 1899-+.
- (149) Dubey, M.; Weidner, T.; Gamble, L. J.; Castner, D. G. *Langmuir* **2010**, *26*, 14747-14754.
- (150) Hsu, C. W.; Liou, H. R.; Su, W. F.; Wang, L. Y. *Journal of Colloid and Interface Science* **2008**, *324*, 236-239.
- (151) Gao, W.; Dickinson, L.; Grozinger, C.; Morin, F. G.; Reven, L. *Langmuir* **1996**, *12*, 6429-6435.
- (152) Gawalt, E. S.; Avaltroni, M. J.; Koch, N.; Schwartz, J. *Langmuir* **2001**, *17*, 5736-5738.
- (153) Guerrero, G.; Mutin, P. H.; Vioux, A. *Chemistry of Materials* **2001**, *13*, 4367-4373.
- (154) Marcinko, S.; Fadeev, A. Y. *Langmuir* **2004**, *20*, 2270-2273.
- (155) Nilsing, M.; Lunell, S.; Persson, P.; Ojamae, L. *Surface Science* **2005**, *582*, 49-60.
- (156) Zorn, G.; Gotman, I.; Gutmanas, E. Y.; Adadi, R.; Salitra, G.; Sukenik, C. N. *Chemistry of Materials* **2005**, *17*, 4218-4226.
- (157) Stromberg, C.; Thissen, P.; Klueppel, I.; Fink, N.; Grundmeier, G. *Electrochimica Acta* **2006**, *52*, 804-815.
- (158) Hotchkiss, P. J.; Malicki, M.; Giordano, A. J.; Armstrong, N. R.; Marder, S. R. *Journal of Materials Chemistry* **2011**, *21*, 3107-3112.
- (159) Zuo, J.; Keil, P.; Valtiner, M.; Thissen, P.; Grundmeier, G. *Surface Science* **2008**, *602*, 3750-3759.
- (160) Szillies, S.; Thissen, P.; Grundmeier, G.; Tabatabai, D.; Feil, F.; Fürbeth, W.; Fink, F. *Corrosion Science*, submitted **2012**.
- (161) Gouzman, I.; Dubey, M.; Carolus, M. D.; Schwartz, J.; Bernasek, S. L. *Surface Science* **2006**, *600*, 773-781.

- (162) Giza, M.; Thissen, P.; Grundmeier, G. *Langmuir* **2008**, *24*, 8688-8694.
- (163) Thissen, P.; Grundmeier, G.; Wippermann, S.; Schmidt, W. G. *Physical Review B* **2009**, *80*.
- (164) Liakos, I. L.; Newman, R. C.; McAlpine, E.; Alexander, M. R. *Langmuir* **2007**, *23*, 995-999.
- (165) Hector, L. G.; Opalka, S. M.; Nitowski, G. A.; Wieserman, L.; Siegel, D. J.; Yu, H.; Adams, J. B. *Surface Science* **2001**, *494*, 1-20.
- (166) Levine, I.; Weber, S. M.; Feldman, Y.; Bendikov, T.; Cohen, H.; Cahen, D.; Vilan, A. *Langmuir*, *28*, 404-415.
- (167) Thissen, P.; Vega, A.; Peixoto, T.; Chabal, Y. J. *Langmuir*, submitted **2012**.
- (168) Klauk, H.; Zschieschang, U.; Pflaum, J.; Halik, M. *Nature* **2007**, *445*, 745-748.
- (169) Zschieschang, U.; Yamamoto, T.; Takimiya, K.; Kuwabara, H.; Ikeda, M.; Sekitani, T.; Someya, T.; Klauk, H. *Advanced Materials*, *23*, 654-+.
- (170) Kitagawa, S.; Matsuda, R. *Coordination Chemistry Reviews* **2007**, *251*, 2490-2509.
- (171) Fischer, R. A.; Woell, C. *Angewandte Chemie-International Edition* **2009**, *48*, 6205-6208.
- (172) Hermes, S.; Schroder, F.; Chelmowski, R.; Woll, C.; Fischer, R. A. *Journal of the American Chemical Society* **2005**, *127*, 13744-13745.
- (173) Shekhah, O.; Wang, H.; Zacher, D.; Fischer, R. A.; Woell, C. *Angewandte Chemie-International Edition* **2009**, *48*, 5038-5041.
- (174) Zacher, D.; Shekhah, O.; Woell, C.; Fischer, R. A. *Chemical Society Reviews* **2009**, *38*, 1418-1429.